Studii şi Cercetări Ştiinţifice
Chimie şi Inginerie Chimică, Biotehnologii, Industrie Alimentară
2024, **25** (1), pp. 071 – 090

Scientific Study & Research
Chemistry & Chemical Engineering, Biotechnology, Food Industry
ISSN 1582-540X

ORIGINAL RESEARCH PAPER

INFLUENCE OF THE ELECTRODE MATERIAL ON ELECTRICAL DISCHARGE MACHINING PROCESS PERFORMANCE

Oana Ghiorghe[1*], Carol Schnakovszky[2], Eugen Herghelegiu[2], Maria Crina Radu[2], Bogdan Alexandru Chirita[2], Nicolae Catalin Tampu[2], Bogdan Nita[1], Petrica Radu[1]

[1]School of Doctoral Studies of the "Vasile Alecsandri" University of Bacau, Calea Marasesti 157, 600115 Bacau, Romania
[2]"Vasile Alecsandri" University of Bacau, Faculty of Engineering, Calea Marasesti 157, 600115 Bacau, Romania

*Corresponding author: oana_ghiorghe@yahoo.com

Received: February, 19, 2024
Accepted: March, 25, 2024

Abstract: Electrical discharge machining is a non-conventional technology widely used to meet the rigors of industrial requirements imposed by the processing of emerging and advanced materials (e.g., geometrical complexity, high dimensional accuracy, and high surface quality). The electrode is one of the most important factors affecting the process performance in terms of production efficiency and machined surface quality. The aim of the current study is to analyze the influence of the electrode material (i.e., copper, tungsten, and brass) on the performance of electrical discharge machining of a C120 die tool steel, quantified by material removal rate, tool wear rate, and electrode wear ratio. The obtained results were statistically processed using the analysis of variance method, to identify the action model of the process control parameters in the perspective of obtaining superior productivity with minimal electrode wear.

Keywords: *analysis of variance (ANOVA), electrode wear ratio (EWR), material removal rate (MRR), tool wear rate (TWR)*

INTRODUCTION

In recent decades, the development of advanced materials with special physicochemical properties intended for the production of components with superior characteristics and complex geometries under conditions of high technical and economic efficiency has led to the development of unconventional processing technologies [1, 2], as their machining by conventional processes has proved to be difficult, costly, or even impossible. Particularly, this concerns the machining of hard and very hard materials (e.g., super alloys [3, 4], carbides [5], composite materials [6, 7], intermetallic compounds [8, 9], ceramics [10], etc.) for the materialization of complex surfaces or the realization of tiny slots, micro-holes, or holes with curvilinear axes, etc., with high accuracy and surface quality.

Electrical discharge machining (EDM) is one such technology. Although it has been more than eight decades since the scientists Boris and Natalia Lazarenko first "drilled" holes in metals using electrical erosion [11, 12], it is only in the last 10-15 years that research in this field has become particularly intensive (Figure 1). The EDM technology is widely used in electronic and electrical engineering, for the production of molds and dies, in aerospace, biomedical, and automotive industries, etc., due to its simple working principle and its inexhaustible technological capacity to meet the requirements mentioned above (i.e., geometric complexity, high dimensional accuracy, and superior surface quality) [13, 14].

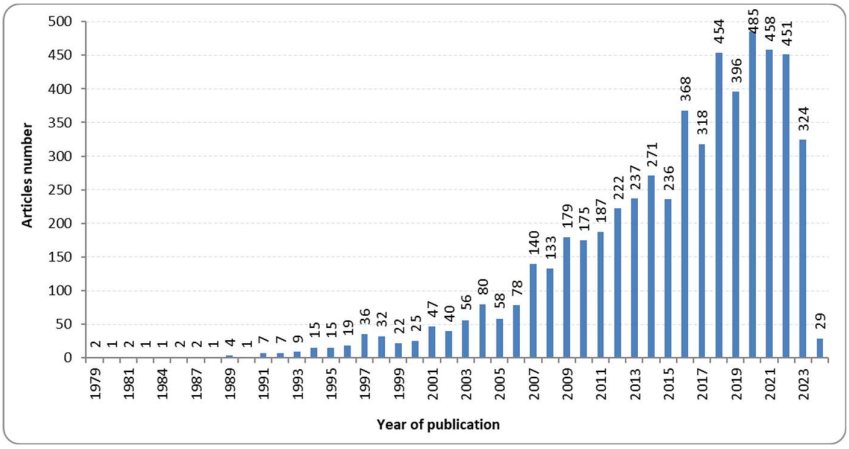

Figure 1. *Publications on EDM: search with "electrical discharge machining" (Title) AND Article (Document Type) available on Clarivate at 26.01.2024*

The machining principle is based on the erosive effect of electrical discharges as impulses conducted between the tool and the workpiece, which are usually connected to the poles of a direct current (DC) source [15].

Between the two electrodes positioned at an initial distance D, there is an electric potential difference V (Figure 2.a), that develops an electric field when they are getting closer, whose intensity I, increases over time (Figure 2.b). When the electric field strength reaches a certain level, the dielectric oil ionizes and breaks down, causing an electric discharge in the gap between the electrodes (Figure 2.c). A plasma bubble is created in the dielectric liquid (Figure 2.d), which very quickly raises the temperature in the area to around 8000 - 12000 ºC and accelerates the dislocation of molten material at

the surface of the two electrodes. When the potential difference between the tool and the workpiece is interrupted, the sudden drop in temperature causes the gas bubble to implode, creating dynamic forces that have the effect of projecting the molten material out of the formed crater (Figure 2.e). The dielectric fluid flushing into the gap solidifies the eroded material and removes it from the machining area (Figure 2.f). These are microscopic phenomena, but they occur rapidly and in very large numbers, so their cumulative effect becomes macroscopic. The machine filtering system cleans the suspended particles from the dielectric fluid [16, 17].

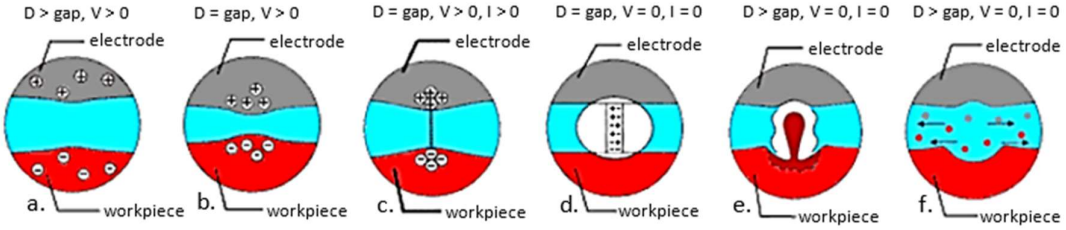

Figure 2. *Phases of the electrical discharge machining process [adapted after 16]*

As there is no direct contact between the electrode and the workpiece during machining, problems such as mechanical stresses and vibrations specific to conventional machining are eliminated [18, 19]. However, EDM has several limitations, including slow MRR, high power consumption [20, 21], and the negative impact of "conventional" dielectric fluids (i.e., hydrocarbon-based or synthetic oils) on the environment and the operator's health and safety [22]. In addition, a white layer (WL) and a heat-affected zone (HAZ) beneath it result from the very high temperatures developed during the machining process [23]. Therefore, an appropriate selection of process parameters (Figure 3) is necessary to increase productivity and improve the quality of processed surfaces.

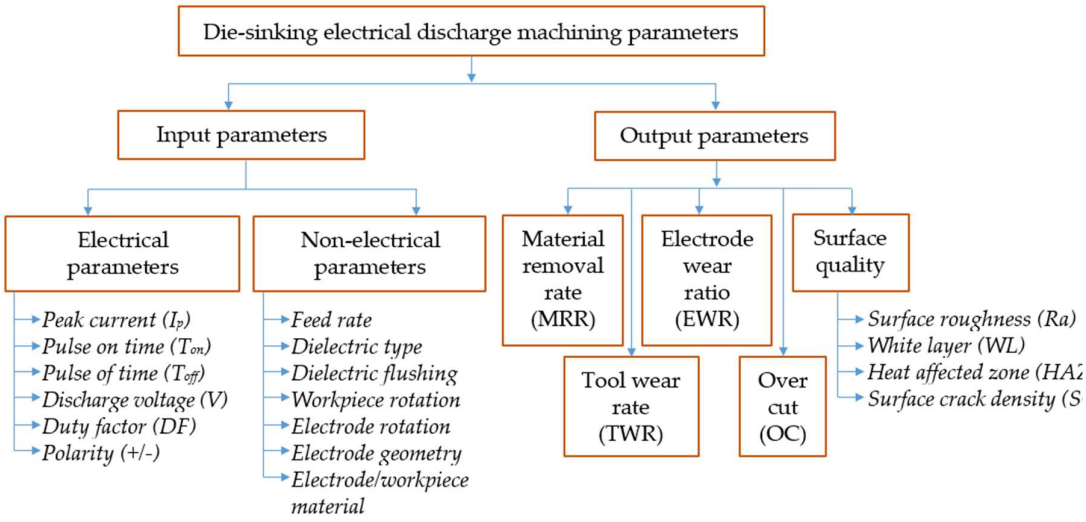

Figure 3. *Factors that affect the die-sinking EDM process performance*

The electrode is one of the most important factors affecting EDM performance since it transmits electrical charges and erodes the workpiece material to a desired shape [17].

Thus, the chemical composition and the physical-mechanical properties of the material from which the electrode is made greatly influence the process productivity and quality: some electrodes erode the workpiece more efficiently but encounter greater wear, while others have slight wear, but the erosion rate is lower [24].
The aim of the current study is to analyze the influence of the electrode material on process performance with the objective of maximizing productivity and minimizing the wear of the electrode, under intensive working regimes conditions. As the two objectives are somehow contradictory, it is very important to identify the action model of the process control parameters [25 – 27]. The electrode type impacts both mechanical features (e.g., MRR, TWR, machined surface quality) as well as the electrical features (e.g., sparking, process stability, etc.) of the EDM process (Table 1) [28 – 46]. A 3^4 full factorial plan was built, and the analysis of variance (ANOVA) method was applied to process the results using Design-Expert.

MATERIALS AND METHODS

Experimental set-up and processed material

Experimental tests were carried out on a KNUTH FEM 110 CNC EDM machine. Four input factors, each with three levels, were used for the factorial plan: electrode material, peak current I_p, pulse on time T_{on}, and pulse off time T_{off} (Table 2). Holes of 2 mm depth have been machined using 10×10 mm electrodes made of copper, tungsten-copper alloy, and brass, with reversed polarity. The OEST FE FLUID 2460 machine mineral oil was used as a dielectric fluid. The chemical composition and properties of the three electrode materials are presented in Tables 3 and 4 [47].
The workpiece material was a C120 (205Cr115) die tool steel, whose chemical composition and properties are given in Tables 5 and 6 [47]. The workpiece dimensions are 100 × 40 × 10 mm.

***Table 1**. Influence of electrode material on EDM process*

Ref.	Year	Electrodes material	Workpiece material	Input parameters						Output parameters				Results
				I_p [A]	T_{on} [µs]	T_{off} [µs]	Discharge voltage [V]	Duty factor [%]	Polarity (+/-)	Dielectric	MRR	TWR	EWR	OC	SQ	
1	2	3	4	5	6	7	8	9	10	11	12	13	14	15	16	17
[28]	2004	Copper; Copper-tungsten; Brass; Aluminum	En-31 tool steel	6; 7.5; 9; 10.5; 12	N/S	N/S	40	N/S	-	EDM oil	√	√		√	√	Copper electrode offers higher MRR, lower OC, lower Ra and less TWR. Aluminum electrode is on second place on performance.
[29]	2007	Graphite, Electrolytic copper; Aluminum	Ti6Al4 V alloy	3; 6; 12; 25	25; 50; 100; 200	25 - - -				kerosene	√	√				Graphite electrode gives the lowest TWR and the highest MRR. Aluminum electrode exhibits the best surface finish.
[30]	2008	Copper; Graphite	XW42 tool steel	3; 6	N/S	N/S	N/S	N/S	+	kerosene	√		√			Copper electrode leads to greater MRR and lower EWR and is more suitable for roughing; graphite electrode - for finishing process.
[31]	2008	Copper; Copper-tungsten	AISI D2 Steel	4.5; 7.5; 10.5	N/S	N/S	N/S	0.5; 0.66; 0.78	+	kerosene	√				√	Copper electrode leads to higher MRR; CW electrode leads to better Ra.
[32]	2009	Copper; Graphite; Copper- graphite	95% pure alumina	1	32	2	N/S	N/S	+ -	N/S	√				√	Graphite EDM-C3 leads to the highest MRR and the best surface finish (Ra).
[33]	2011	Copper with different shapes	AISI H13 steel	4; 5; 6; 7	25; 50; 100; 200	3.2; 6.4; 13; 25	80; 120; 160; 200		+	N/S	√				√	Square and rectangle electrode shapes lead to better results.

1	2	3	4	5	6	7	8	9	10	11	12	13	14	15	16	17
[34]	2013	Copper: Brass: Tungsten carbide	AISI 202 stainless steel	9; 12; 15	N/S	N/S	40; 60; 80	0.4; 0.6; 0.8	N/S	N/S	√		√		√	Copper electrode leads to a higher MRR, whereas tungsten carbide electrode allows a better surface finish.
[35]	2014	Copper; Copper–tungsten; Graphite	Ti-5Al-2.5Sn alloy	15; 29; 2	180; 320; 95	120	N/S	N/S	N/S	N/S					√	Copper–tungsten electrode leads to the finest processed surface, while graphite delivers worst surface characteristics.
[36]	2015	Dura graphite 11; Poco graphite EDMC-3	DIN 1.2080; DIN 1.2379	15; 30; 50	20; 100; 180	N/S	N/S	N/S	N/S	N/S					√	Dura graphite leads to a higher Ra. Poco graphite leads to higher residual stresses.
[37]	2016	Copper (circular and square shaped electrodes)	6351 aluminium alloy	5; 10; 15	50; 75; 100	N/S	40-50	4; 6; 8		EDM oil			√	√	√	Circular electrode leads to less EWR and OC as well as a better surface finish than square electrode.
[38]	2018	Copper; Brass; Zinc	Ti-5Al-2.5Sn alloy	10; 15; 20	100; 200; 300	N/S	40; 50; 60	60; 75; 90	N/S	N/S	√	√			√	Brass and zinc electrodes lead to a higher MRR than copper electrode. Copper electrode exhibits less tool wear and a better surface finish, followed by brass and zinc electrodes.
[39]	2018	Tungsten: Copper (normal and cryogenically treated)	Ti-6Al-4V alloy	6; 8; 10	300	N/S	25	85	+	EDM oil grade 30	√				√	Cryogenically treated Copper electrode leads to increased MRR, improved surface finish, and reduced wear.
[40]	2019	Copper; Brass; Graphite	AISI H13 die steel	2; 6; 14	50; 150; 500	N/S	N/S	50	-	kerosene	√		√		√	Copper electrode leads to the highest. MRR and lowest EWR; Brass electrode leads to the lowest SR.

1	2	3	4	5	6	7	8	9	10	11	12	13	14	15	16	17
[41]	2020	Unprocessed and ECAP copper	AISI H13 die steel	6; 12; 18; 24	100; 200; 500; 1000	N/S	N/S	N/S	N/S	EDM oil grade 30	√	√			√	Unprocessed copper electrode leads to higher MRR as well as higher TWR and worse SQ. Triple ECAP passed copper electrode leads to an improvement in SQ of 50% and a reduction in TWR of 55%.
[42]	2020	Graphite electrodes with different flushing patterns	Carbon steel (A3)	400; 600; 800; 1000	3; 5; 7; 9	1	90	N/S	+	N/S	√	√				Linear flushing patterns lead to a higher MRR. A high number of small flushing holes leads to the highest TWR.
[43]	2021	Graphite; Copper; Brass	HcHcr D2 steel	3; 6; 9	50; 75; 100	50	230	N/S	+	Kerosene; Distilled water	√	√			√	Graphite electrode leads to higher MRR, lower SR, and TWR when distilled water is used as a dielectric.
[44]	2021 2022	Single-channel electrode; Porous electrode	Ti6Al4V alloy	64	560	100	100	N/S	-	EDM oil	√	√			√	Porous electrode leads to higher machining efficiency than traditional EDM.
[45]	2023	Copper; Brass; Tungsten carbide	Titanium α- β alloy	9; 12; 15	N/S	N/S	40; 79; 90	0.4; 0.6; 0.8	N/S	EDM oil	√		√		√	Copper electrode leads to the highest MRR. Tungsten carbide electrode leads to the best surface topography.
[46]	2023	Sub-zero treated and untreated copper electrodes	Ti-6Al-4V alloy	12; 18; 24	50; 100; 150	N/S	50; 60; 70	50	+	EDM 3 Oil	√	√			√	Sub-zero treated electrodes lead to higher MRR, lower TWR and better-quality surface.

Polarity is considered positive (+) when the workpiece is positive, and the electrode is negative. SR or Ra - surface roughness; ECAP - equal channel angular pressed copper (single, twice, and third passes through the ECAP die); N/S - not specified.

Table 2 *Variation levels of the experimental parameters*

Process Variables	**Variation Levels**					
	Level 1		**Level 2**		**Level 3**	
	Coded	**Value**	**Coded**	**Value**	**Coded**	**Value**
Peak current, I_p [A]	**10**	*11.4*	**15**	*57.3*	**20**	*114*
Pulse on time, T_{on} [µs]	**9**	*13*	**29**	*380*	**35**	*600*
Pulse off time, T_{off} [µs]	**10**	*18*	**20**	*120*	**30**	*420*

Table 3 *Chemical composition of the electrode materials* [47]

Electrolytic copper Cu 99.9						
Cu [%]		**O [%]**		**Pb [%]**		**Bi [%]**
99.9		0.04		0.005		0.0005
Tungsten-copper WCu 75/25						
Cu [%]		**W [%]**		**Additive [max.%]**		
25±2		Remaining		1		
Brass CuZn39Pb2						
Fe [%]	**Ni [%]**	**Al [%]**	**Cu [%]**	**Pb [%]**	**Sn [%]**	**Others [%]**
max 0.3	max 0.3	max 0.05	59 - 60	1.6 - 2.5	max 0.3	total 0.2

Table 4 *Properties of the electrode materials* [47]

Properties / Material	**Electrolytic copper Cu 99.9**	**Tungsten-copper WCu 75/25**	**Brass CuZn39Pb2**
Tensile strength [MPa]	235–395	585–654	360–440
Modulus of elasticity [GPa]	115	260	96
Density [$g \cdot cm^{-3}$]	8.9	14.3	8.46
Hardness [HB]	70–120	89–102	86–115
Electrical conductivity [$m \cdot \Omega^{-1} \cdot mm^{-2}$]	100	41–48	24
Thermal conductivity [$W \cdot (m \cdot K)^{-1}$]	388	190	110

Table 5 *Chemical composition of the workpiece material* [47]

C [%]	**Si [%]**	**Mn [%]**	**P [%]**	**S [%]**	**Cr [%]**	**Ni [%]**	**Cu [%]**
1.15-1.25	0.1-0.3	0.1-0.4	<0.030	<0.030	-	-	-

Table 6 *Properties of the workpiece material* [47]

Tensile strength [MPa]	**Modulus of elasticity [GPa]**	**Density [$g \cdot cm^{-3}$]**	**Hardness [HB]**	**Electrical conductivity [% IACS]**	**Thermal conductivity [$W \cdot (m \cdot K)^{-1}$]**
925	207	7.7	241	3.5	31

Output parameters

Material removal rate (MRR), tool wear rate (TWR), and electrode wear ratio (EWR) were analyzed as output parameters to quantify the performance of the EDM process under the condition of the previously mentioned input parameters.

MRR and TWR express the volume of material removed from the workpiece (V_m) and tool (V_t), respectively, with respect to the machining time (t) and can be determined with the following equations [48, 49]:

$$MRR = \frac{V_m}{\rho_m \cdot t} \quad (mm^3 \cdot min^{-1}) \tag{1}$$

$$TWR = \frac{V_t}{\rho_t \cdot t} \quad (mm^3 \cdot min^{-1}) \tag{2}$$

where ρ_m and ρ_t represent the density of workpiece material, and tool material, respectively.
EWR is the ratio of electrode wear to the workpiece wear after machining and can be expressed as [49]:

$$EWR = \frac{W_t}{W_m} \times 100 \quad (\%) \tag{3}$$

where W_t is the wear weight of the tool, and W_m is the wear weight of the workpiece.
The weights of the workpiece and the tools before and after each cavity machining were measured with a microgram precision balance (RADWAG, Radom, Poland).

Statistical analysis

ANOVA models were generated in Design Expert using an algorithm for the automatic selection of the terms based on their statistical significance, which is measured by p-value. If the p-value is lower than 0.05 the term is considered significant. However, some non-significant terms may be included in the model if they are involved in statistically significant interactions to preserve the hierarchy of the model.

RESULTS AND DISCUSSION

Material removal rate (MRR) analysis

The results from ANOVA (Table 7) revealed that the most influential factors on material removal rate (MRR) are the peak current I_p (26.32 %), the electrode material (22.55 %), pulse on time T_{on} (14.81 %), as well as their interactions: electrode material-peak current (11.75 %), electrode material-pulse on time (9.84 %), peak current-pulse on time (5.76 %), and electrode material-peak current-pulse on time (5.31 %). The model covers 99.36 % of the response variability and there is a very good agreement between the correlation coefficients (Adj.R^2 and Pred.R^2).
Figure 4 illustrates the effects of the input factors on MRR. The highest productivity is obtained with the Cu 99.9 electrode, followed by the WCu 75/25 electrode, and the CuZn39Pb2 electrode. MRR raises with the increase of the peak current and the pulse on time parameters, respectively. On the other hand, the pulse off time does not influence MRR. However, there are some particularities dictated by the electrode material, concerning the effect of the peak current and pulse on time on MRR. When the EDM is made with the copper electrode the increase of the peak current leads to a constant rise of the MRR, whereas at the increase of the pulse on time there is a threshold for T_{on} = 29 and after that, the MRR does not improve (Figure 4.a). For the tungsten electrode, there are threshold values for both the peak current (I_p = 15) and the pulse on time (T_{on} = 29) in the evolution of the MRR (Figure 4.b). For the brass electrode, MRR is not affected by the modifications of peak current and pulse on time (Figure 4.c).

Table 7. *ANOVA results for MRR*

Source	Sum of squares	df	Mean square	F-value	p-value
Model	1.221E+05	56	2181.16	66.38	< 0.0001
A - Electrode material	27713.65	2	13856.83	421.70	< 0.0001
B - Peak current, I_p	32344.14	2	16172.07	492.16	< 0.0001
C - Pulse on time, T_{on}	18199.41	2	9099.70	276.93	< 0.0001
D - Pulse off time, T_{off}	52.68	2	26.34	0.8017	0.4602
AB	14441.66	4	3610.42	109.88	< 0.0001
AC	12095.25	4	3023.81	92.02	< 0.0001
AD	100.38	4	25.09	0.7637	0.5592
BC	7077.25	4	1769.31	53.85	< 0.0001
BD	205.45	4	51.36	1.56	0.2163
CD	1795.48	4	448.87	13.66	< 0.0001
ABC	6523.48	8	815.43	24.82	< 0.0001
ACD	534.39	8	66.80	2.03	0.0856
BCD	1061.75	8	132.72	4.04	0.0037
Residual	788.62	24	32.86		
Cor Total	1.229E+05	80			
$R^2 = 0.9936$	Adj.$R^2 = 0.9786$			Pred.$R^2 = 0.9269$	

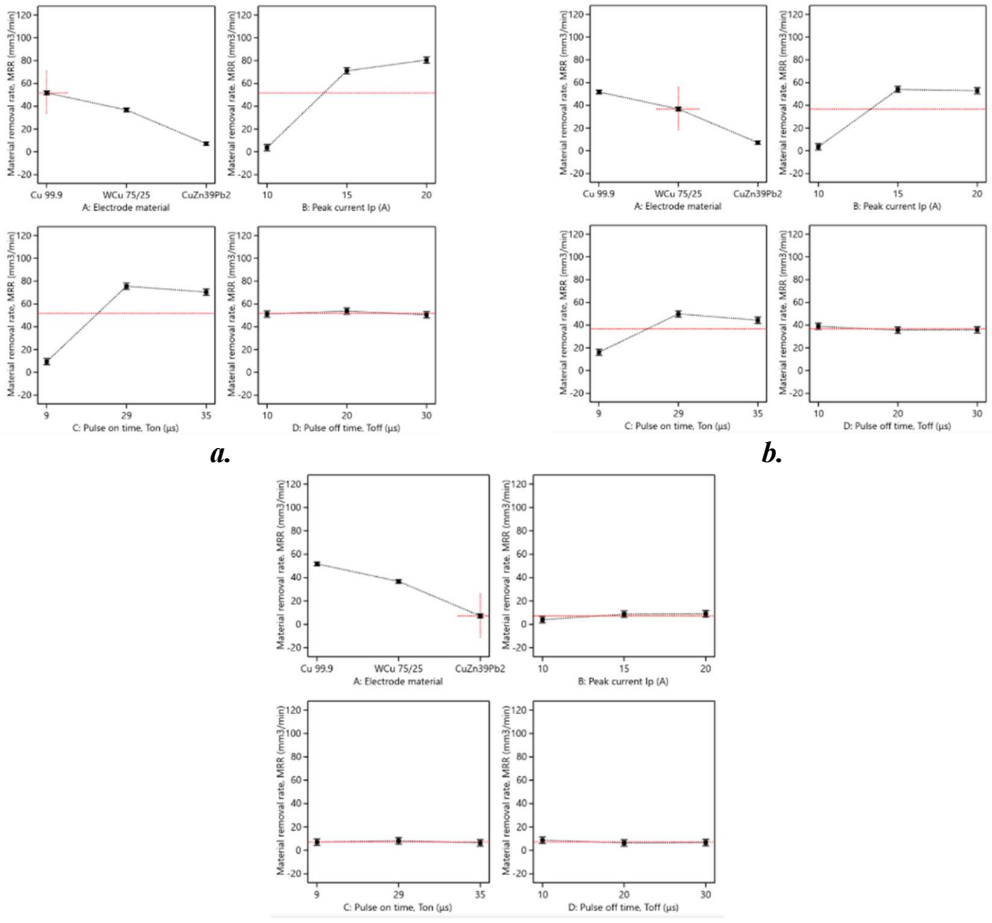

a. ***b.***

c.

Figure 4. *Main effects of input factors on MRR:*
a. Cu 99.9 electrode; b. WCu 75/25 electrode; c. CuZn39Pb2 electrode

The combined effect of the electrode material and the peak current on MRR is presented in Figure 5. It shows that for the lowest peak current, MRR values remain almost constant and are not affected by the electrode material. The productivity of the EDM process increases the most when the copper electrode is used, and the peak current is raised to higher values. For the tungsten electrode, there is a significant leap of MRR when the peak current increases from 10 to 15, but after that MRR remains approximately the same. In the case of the brass electrode MRR is virtually unaffected by the increase of the peak current.

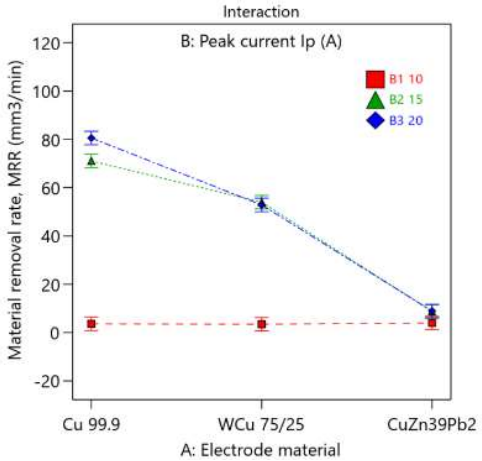

Figure 5. *Effect of electrode material – peak current interaction on MRR*

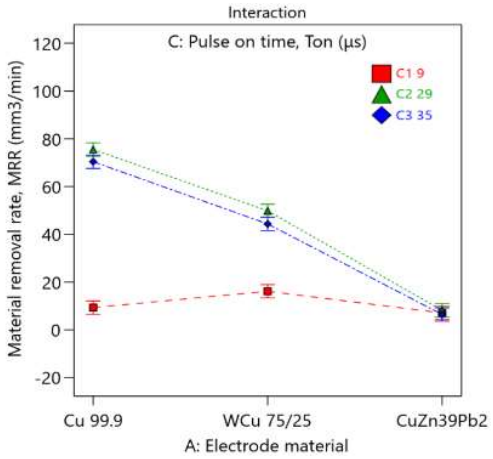

Figure 6. *Effect of electrode material – pulse on time interaction on MRR*

Figure 6 presents the effect of the electrode material–pulse on time interaction on MRR. It can be observed that for the lowest value of the pulse on time (T_{on} = 9), MRR has a very small variation when EDM is performed with different electrode materials. The increase of the pulse on time duration is the most effective for the copper electrode, followed by the tungsten electrode, whereas, for the brass electrode, the variations are negligible. However, it can be clearly seen that the increase of the pulse on time is effective only to a certain extent, as the MRR values for T_{on} = 35 are lower than the ones for T_{on} = 29, regardless of the electrode material.

Tool wear rate (TWR) analysis

For the tool wear rate (TWR) the analysis of variation has shown that the most important factors are the electrode material, with an influence of 52.31 %, followed by the peak current, with 15.73 %, and their interaction electrode material-peak current with 15.58 % (Table 8). The model has good correlation coefficients, as the difference between Adj.R^2 and Pred.R^2 is less than 0.2.

Table 8. *ANOVA results for TWR*

Source	Sum of squares	df	Mean square	F-value	p-value
Model	2509.77	20	125.49	20.21	< 0.0001
A - Electrode material	1494.90	2	747.45	120.37	< 0.0001
B - Peak current, I_p	449.50	2	224.75	36.20	< 0.0001
C - Pulse on time, T_{on}	23.09	2	11.54	1.86	0.1653
D - Pulse off time, T_{off}	4.75	2	2.37	0.3825	0.6839
AB	445.16	4	111.29	17.92	< 0.0001
AC	81.64	4	20.41	3.29	0.0172
CD	63.30	4	15.83	2.55	0.0492
Residual	347.73	56	6.21		
Cor Total	2857.50	76			
$R^2 = 0.8783$	$Adj.R^2 = 0.8349$			$Pred.R^2 = 0.7582$	

The main effects of the input factors on the tool wear rate TWR are presented in Figure 7. As can be observed, the lowest wear rate was reported for the WCu 75/25 electrode, and the highest was for the CuZn39Pb2 electrode. TWR intensifies with the increase of the peak current I_p, but it is highly dependent on the electrode material. The results from ANOVA have shown that TWR is not significantly influenced by pulse on time and pulse off time, which can also be seen in Figure 7.

A clarification must be made concerning some of the TWR values recorded for the copper electrodes and tungsten electrodes. When the pulse current has the lowest value ($I_p = 10$) and the pulse on time values are high ($T_{on} = 29$ and $T_{on} = 35$) negative values were recorded for TWR. This can be explained by the development of material depositions on the electrode surface that are higher than the effective wear of the electrode. Because of this phenomenon, TWR exhibits a decreasing rate with pulse on time, which can be seen in Figures 7.a and 7.b.

The effect of the interaction electrode material-peak current on TWR is presented in Figure 8. The lowest wear rate appears for the combination of Cu 99.9 electrode and the lowest peak current Ip = 10. The highest TWR values result when brass electrodes are used with high peak currents. The tungsten electrodes exhibit the lowest variability of the wear rate.

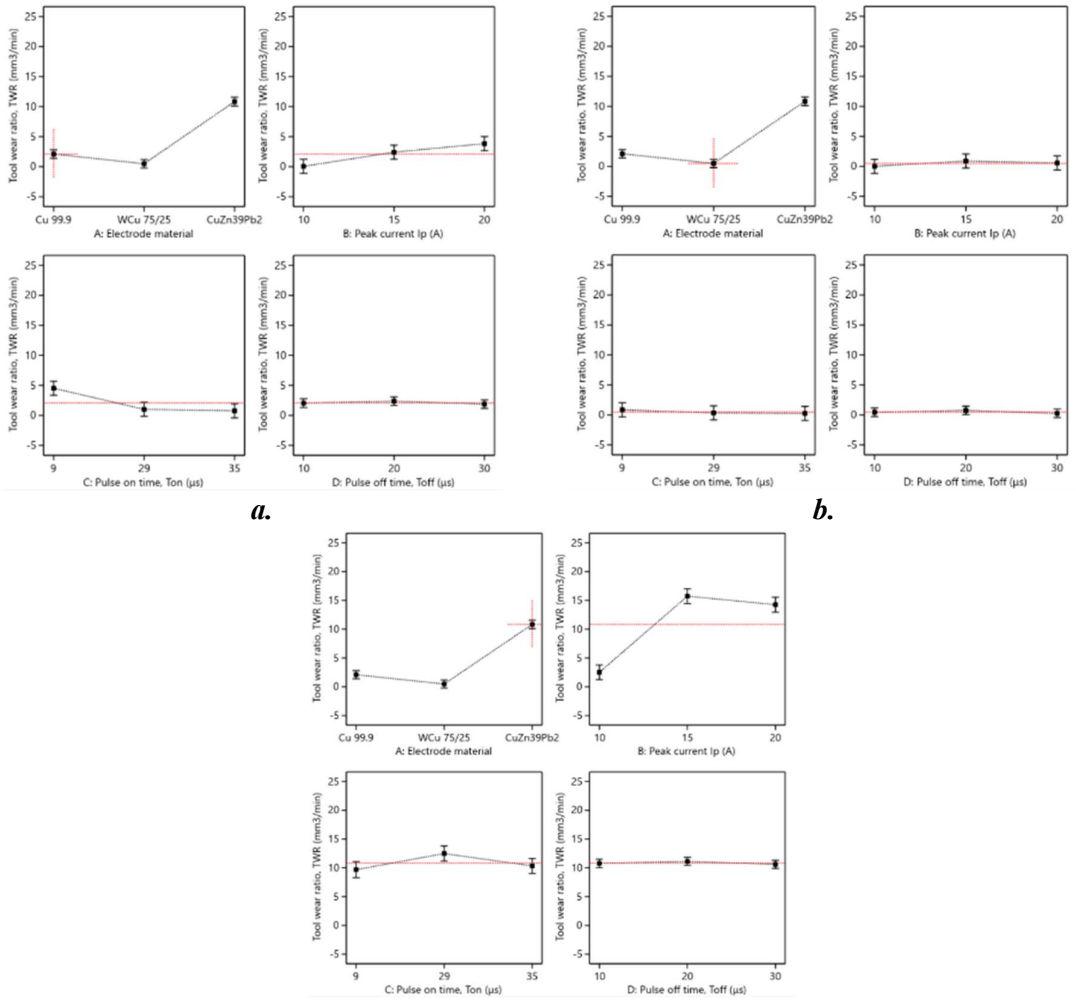

Figure 7. *Main effects of input factors on TWR:*
a. Cu 99.9 electrode; b. WCu 75/25 electrode; c. CuZn39Pb2 electrode

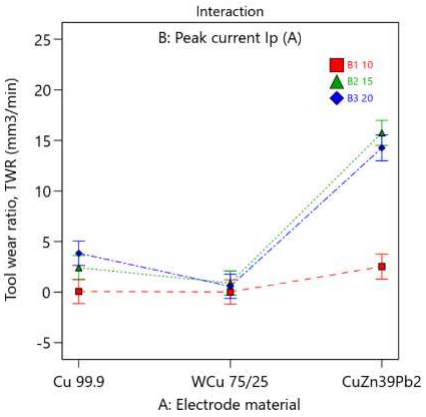

Figure 8. *Effect of electrode material – peak current interaction on TWR*

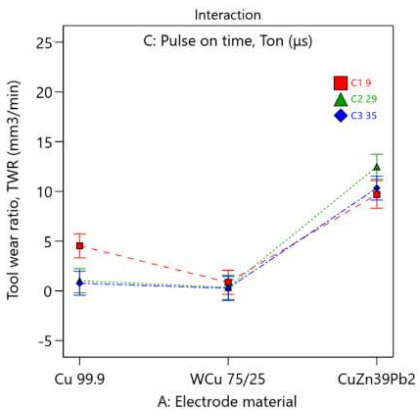

Figure 9. *Effect of electrode material – pulse on time interaction on TWR*

To sustain the hypothesis of material depositions on the electrode when the TWR is negative, one of the copper electrodes was analyzed with a TESCAN MIRA scanning electron microscope (SEM). Figure 10 shows an image of the electrode surface where the particles of the deposed material are clearly visible. The energy-dispersive X-ray spectroscopy (EDS) analyses (Figure 11) have indicated the presence of elements such as iron (Fe), carbon (C), chrome (Cr), and traces of rubidium (Rb), that are constituents of the workpiece material. Particles detached from the workpiece by the electrical discharge have adhered to the surface of the electrode contributing thus to the increase of the electrode weight.

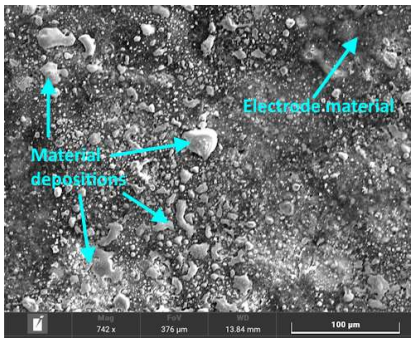

Figure 10. *SEM image of the electrode surface*

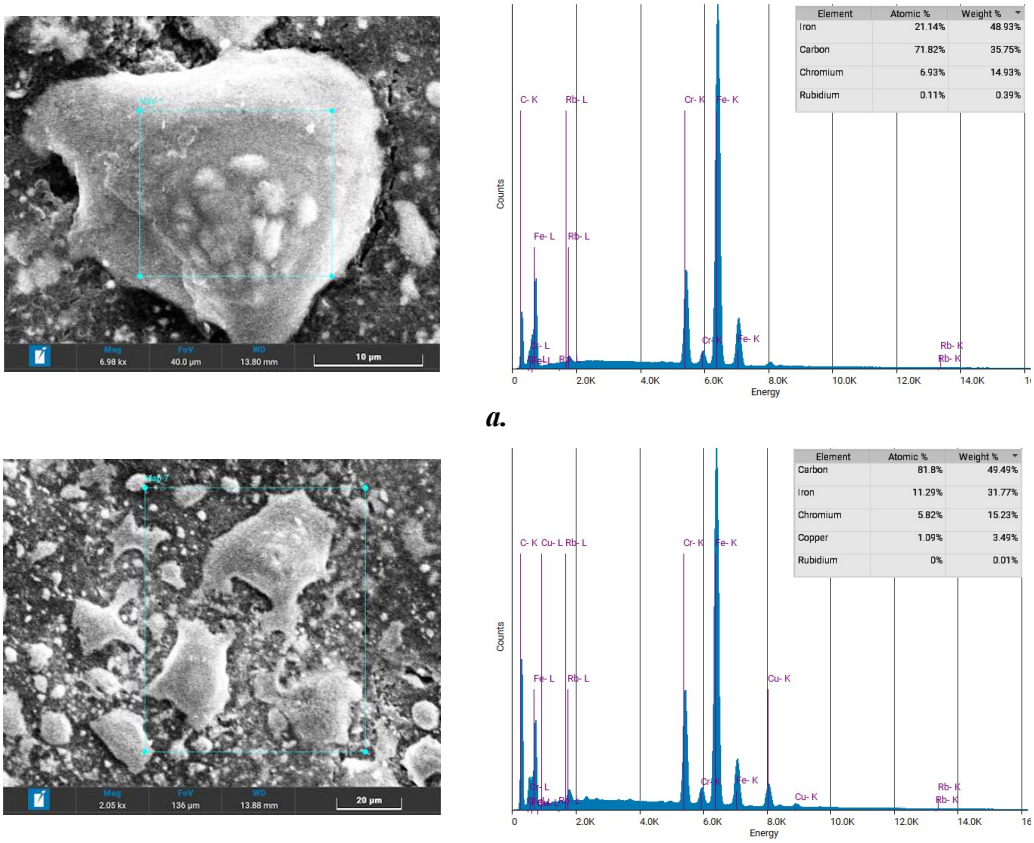

Figure 11. *Details from SEM image and EDS analysis results*

Electrode wear ratio (EWR)

In the case of electrode wear ratio (EWR), ANOVA (Table 9) has shown that the electrode material has the largest influence, with a proportion of 66.95 % from total variability. Among the other significant factors, the pulse on time has a 6.40 % influence, followed by the peak current with a 4.74 % influence. The most important interactions are electrode material-peak current with 6.19 % influence, and electrode material-pulse on time-pulse off time with 5.30 % influence. The model can explain 97.45 % of the response variability and there is a good agreement between Adj.R^2 and Pred.R^2.

Table 9. *ANOVA results for EWR*

Source	Sum of squares	df	Mean square	F-value	p-value
Model	9.381E+05	44	21320.58	31.30	< 0.0001
A - Electrode material	6.445E+05	2	3.223E+05	473.04	< 0.0001
B - Peak current, I_p	45660.53	2	22830.27	33.51	< 0.0001
C - Pulse on time, T_{on}	61608.40	2	30804.20	45.22	< 0.0001
D - Pulse off time, T_{off}	2987.77	2	1493.88	2.19	0.1263
AB	59578.94	4	14894.74	21.86	< 0.0001
AC	29525.41	4	7381.35	10.84	< 0.0001
AD	17561.52	4	4390.38	6.44	0.0005
BC	884.36	4	221.09	0.3245	0.8597
CD	11521.05	4	2880.26	4.23	0.0066
ABC	13245.04	8	1655.63	2.43	0.0326
ACD	51023.42	8	6377.93	9.36	< 0.0001
Residual	24524.77	36	681.24		
Cor Total	9.626E+05	80			
R^2 = 0.9745	Adj.R^2 = 0.9434			Pred.R^2 = 0.8710	

Figure 12 shows the main effect of the input factors on EWR. Because EWR is calculated as a ratio between the electrode wear and the quantity of material eroded from the workpiece, the main factor of influence is the electrode material, while the peak current and pulse on time have a much lower effect, as mentioned earlier. The brass electrode has an increased wear, compared to the other two electrode materials, and the influence of peak current and pulse on time, respectively, is more visible in this case (Figure 12.c).

Figure 13 illustrates the effect of electrode material-peak current interaction on EWR. It shows that the increase of the peak current is effective only to a certain extent, as the EWR does not modify after I_p passes above 15, regardless of the electrode material.

A similar situation can be observed for the effect of electrode material-pulse on time interaction (Figure 14), as EWR does not change after T_{on} increases above 29 for all electrodes.

The interaction between the electrode material and the pulse off time resembles the previous interactions and it is more noticeable for the CuZn39Pb2 electrode (Figure 15).

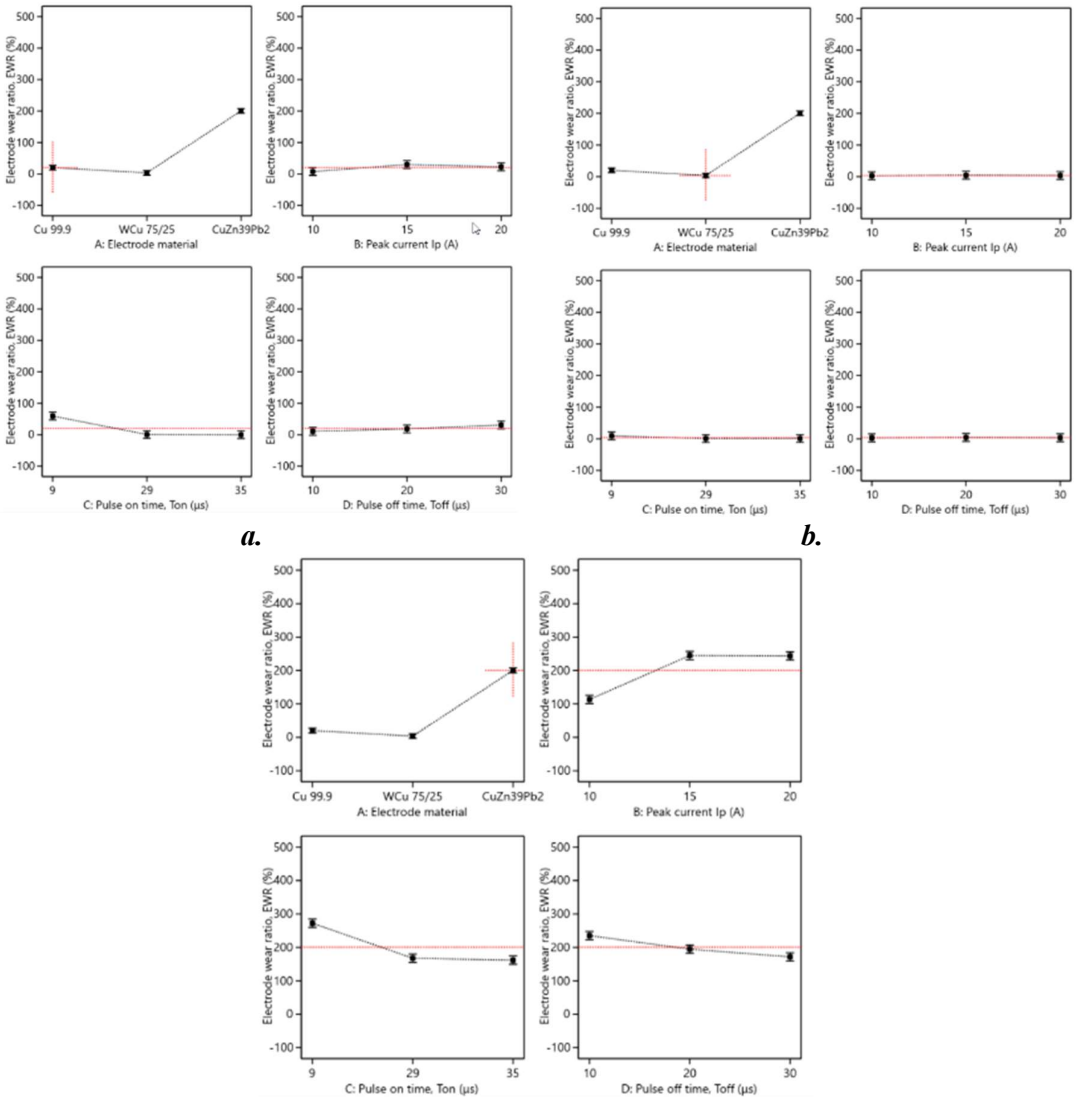

Figure 12. *Main effects of input factors on EWR:*
a. Cu 99.9 electrode; b. WCu 75/25 electrode; c. CuZn39Pb2 electrode

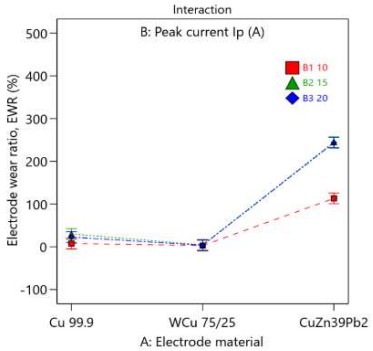

Figure 13. *Effect of electrode material – peak current interaction on EWR*

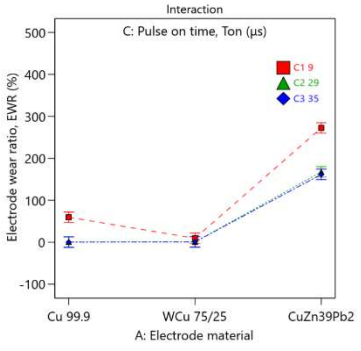

Figure 14. *Effect of electrode material – pulse on time interaction on EWR*

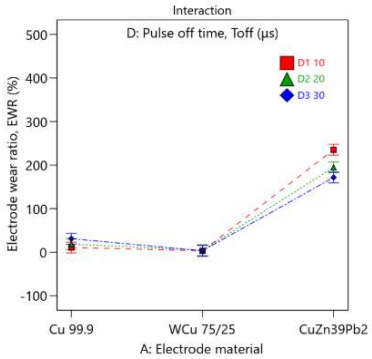

Figure 15. *Effect of electrode material – pulse off time interaction on EWR*

CONCLUSIONS

The present paper aimed to highlight the effect of the electrode material on the productivity of the EDM process (by MRR), and on the electrode wear (TWR, EWR) under intensive processing parameters. The study was conducted according to a 3^4 full factorial design.

The following conclusions can be formulated, based on the obtained results:

- The maximum MRR was obtained by using the copper Cu 99.9 electrodes.
- The use of the brass CuZn39Pb2 electrodes resulted in the lowest process productivity.
- The tungsten alloy WCu 75/25 electrodes presented the lowest wear rate, followed closely by the copper electrodes.
- The brass electrodes exhibited an average wear rate 22.25 times higher than the tungsten electrodes.
- The study has also highlighted the existence of some threshold values for the peak current I_p and pulse on time T_{on} up to which the improvement of productivity and wear rate is obtained.

In conclusion, for the EDM processing of the C120 die tool steel it is recommended the use of the copper Cu 99.9 or tungsten WCu 75/25 electrodes.

REFERENCES

1. Radu, M.C., Schnakovszky, C., Herghelegiu, E., Tampu, N.C., Zichil, V.: Comparative analysis of the processing accuracy of high strength metal sheets by AWJ, laser and plasma in: *IOP Conference Series-Materials Science and Engineering*, Ed. IOP Publishing, **2016**, **145**, 022034, doi:10.1088/1757-899X/145/2/022034;
2. Sarala Rubi, C., Prakash, J.U., Juliyana, S.J., Čep, R., Salunkhe, S., Kouril, K., Ramdas Gawade, S.: Comprehensive Review on Wire Electrical Discharge Machining: A Nontraditional Material Removal Process, *Frontiers of Mechanical Engineering*, **2024**, **10**, 1322605, doi:10.3389/fmech.2024.1322605;
3. Herghelegiu, E., Schnakovszky, C., Radu, M.C., Tampu, N.C., Zichil, V.: Comparative study on the processing of armour steels with various unconventional technologies in: IOP Conference Series-Materials Science and Engineering, Ed. IOP Publishing, **2017**, **227**, 012058, doi:10.1088/1757-899X/227/1/012058;

4. Vora, J., Khanna, S., Chaudhari, R., Patel, V.K., Paneliya, S., Pimenov, D.Y., Giasin, K.: Chander Prakash, Machining parameter optimization and experimental investigations of nano-graphene mixed electrical discharge machining of nitinol shape memory alloy, *Journal of Materials Research and Technology*, **2022**, **19**, 653-668, doi:10.1016/j.jmrt.2022.05.076;
5. Klocke, F., Chrubasik, L., Klink, A., Hensgen, L.: Analysis of Fundamental Process Characteristics for Sinking-EDM of Cemented Carbides as a Function of Polarity, *Procedia CIRP*, **2018**, **68**, 313-318, doi:10.1016/j.procir.2017.12.070;
6. Sidhu, S.S., Ablyaz, T.R., Bains, P.S., Muratov, K.R., Shlykov, E.S., Shiryaev, V.V.: Parametric Optimization of Electric Discharge Machining of Metal Matrix Composites Using Analytic Hierarchy Process, *Micromachines*, **2021**, **12**, 1289, doi:10.3390/mi12111289;
7. Channi, A.S., Bains, H.S., Grewal, J.S., Kumar, R., Buddhi, D.: Exploring the Application Sphere of Electrical Discharge Machining in Composite Materials Considering Surface Features: A Content Analysis, *International Journal on Interactive Design and Manufacturing*, **2023**, **17**, 2095-2114, doi:10.1007/s12008-022-01060-3;
8. Radu, P., Schnakovszky. C., Herghelegiu. E., García-Martínez. E., Miguel, V.: Study on the Current State of Research in the Field of Titanium Aluminides Milling Processes, *Key Engineering Materials*, **2023**, **955**, 3–13, doi:10.4028/p-aith0z;
9. García-Martínez, E., Miguel, V., Martínez-Martínez, A., Coello, J., Naranjo, J.A., Manjabacas, M.C.: Optimization of the Dry Turning Process of Ti48Al2Cr2Nb Aluminide Based on the Cutting Tool Configuration, *Materials*, **2022**, **15** (4), 1472, doi:10.3390/ma15041472;
10. Grigoriev, S.N., Hamdy, K., Volosova, M.A., Okunkova, A.A., Fedorov, S.V.: Electrical Discharge Machining of Oxide and Nitride Ceramics: A Review, *Materials & Design*, **2021**, **209**, 109965, doi:10.1016/j.matdes.2021.109965;
11. Bologa, M.: Academicianul Boris Lazarenco – Fondatorul Metodei Electroeroziunii, *Enciclopedica. Revistă de Istorie a Științei și Studii Enciclopedice*, **2015**, **2** (9), 5-7;
12. Bologa, M.: Savantul Care a Revoluționat Domeniul Prelucrării Metalelor la Aniversarea a 110-a a Academicianului Boris Lazarenko, *Istoria Științei*, **2020**, **3**, 95-101;
13. Chaudhury, P., Samantaray, S.: A Comparative Study of Different Dielectric Medium for Sustainable EDM of Non-Conductive Material by Electro-Thermal Modelling, *Materials Today: Proceedings*, **2021**, **41** (2), 437-444, doi:10.1016/j.matpr.2020.10.162;
14. Kamenskikh, A.A., Muratov, K.R., Shlykov, E.S., Sidhu, S.S., Mahajan, A., Kuznetsova, Y.S., Ablyaz, T.R.: Recent Trends and Developments in the Electrical Discharge Machining Industry: A Review, *Journal of Manufacturing and Materials Processing*, **2023**, **7**, 204, doi:10.3390/jmmp7060204;
15. Saffaran, A., Azadi Moghaddam, M., Kolahan, F.: Optimization of backpropagation Neural Network-Based Models in EDM Process Using Particle Swarm Optimization and Simulated Annealing Algorithms, *Journal of the Brazilian Society of Mechanical Sciences and Engineering*, **2020**, **42**, 73, doi: 10.1007/s40430-019-2149-1;
16. https://charmilles.ro/electroeroziune.html, Electroeroziune, accessed February 2, 2024;
17. Sommer, C., Sommer, S.: *Complete EDM Handbook*, Second Edition, Advance Publications, New York, **2017**, 137-159;
18. Zhou, M., Hu, T., Mu, X., Zhao, M., Yang, J., Ye, Q., Xu, P., Yang, L., Xin, F.: Significant Step towards Efficient Electrical Discharge Machining Titanium Alloys, *The International Journal of Advanced Manufacturing Technology*, **2023**, **27**, 3905–3918, doi:10.1007/s00170-023-11767-6;
19. Navas, V.G., Ferreres, I., Maranon, J.A., Garcia-Rosales, G., Gil Sevillano, J.: Electro-Discharge Machining (Edm) Versus Hard Turning and Grinding—Comparison of Residual Stresses and Surface Integrity Generated in AISI O1 Tool Steel, *Journal of Materials Processing Technology*, **2008**, **195**, 186-194, doi:10.1016/j.jmatprotec.2007.04.131;
20. Hasan, A., Mushtaq, R.T., Khan, A.M., Anwar, S.: Parametric Investigation of the Effects of Electrical Discharge Machining on Plain D2 Steel, *Metals*, **2023**, **13**, 1964, doi:10.3390/met13121964;

21. Abu Quedeiri, J.B., Saleh, A., Ziout, A., Mourad, A.-H.I., Abidi, M.H., Elkaseer, A.: Advanced Electric Discharge Machining of Stainless Steels: Assessment of the State of the Art, Gaps and Future Prospect, *Materials*, **2019**, **12** (6), 907, doi:10.3390/ma12060907;
22. Radu, M.-C., Tampu, R., Nedeff, V., Patriciu, O.-I., Schnakovszky, C., Herghelegiu, E., Experimental Investigation of Stability of Vegetable Oils Used as Dielectric Fluids for Electrical Discharge Machining, *Processes*, **2020**, **8** (9), 1187, doi:10.3390/pr8091187;
23. Karmiris-Obratanski, P., Papazoglou, E.L., Leszczynska-Madej, B., Karkalos, N.E., Markopoulos, A.P.: An Optimalization Study on the Surface Texture and Machining Parameters of 60CrMoV18-5 Steel by EDM, *Materials*, **2022**, **15** (10), 3559, doi:10.3390/ma15103559;
24. Garba, E., Abdul-Rani, A.M., Yunus N.A., Abdu Aliyu, A.A., Gul, I.A., Al-Amin, M., Aliyu, R.: A Review of Electrode Manufacturing Methods for Electrical Discharge Machining: Current Status and Future Perspectives for Surface Alloying, *Machines*, **2023**, **11**, 906, doi:10.3390/machines11090906;
25. Patel, K.M., Pandey, M.P., Paruchuri, V.R.: Determination of an Optimum Parametric Combination Using a Surface Roughness Prediction Model for EDM of Al_2O_3/SiC_w/TiC Ceramic Composite, *Materials and Manufacturing Processes*, **2009**, **24** (6), 675-682, doi:10.1080/10426910902769319;
26. Huu Phan, N., Muthuramalingam, T.: Multi Criteria Decision Making of Vibration Assisted EDM Process Parameters on Machining Silicon Steel Using Taguchi-DEAR Methodology, *Silicon*, **2021**, **13**, 1879–1885, doi:10.1007/s12633-020-00573-4;
27. Karthik Pandiyan, G., Prabaharan, T., Jafrey Daniel James, D., Sivalingam, V.: Machinability Analysis and Optimization of Electrical Discharge Machining in AA6061-T6/15wt.% SiC Composite by the Multi-criteria Decision-Making Approach, *Journal of Materials Engineering and Performance*, **2022**, **31**, 3741-3752, doi:10.1007/s11665-021-06511-8;
28. Singh, S., Maheshwari, S., Pandey, P.C.: Some Investigations into the Electric Discharge Machining of Hardened Tool Steel Using Different Electrode Materials, *Journal of Materials Processing Technology*, **2004**, **149**, 272-277, doi:10.1016/j.jmatprotec.2003.11.046;
29. Hascalik, A., Caydas, U.: Electrical Discharge Machining of Titanium Alloy (Ti–6Al–4V), *Applied Surface Science*, **2007**, **253**, 9007-9016, doi:10.1016/j.apsusc.2007.05.031;
30. Che Haron, C.H., Ghani, J.A., Burhanuddin, Y., Seong, Y.K., Swee, C.Y.: Copper and Graphite Electrodes Performance in Electrical-Discharge Machining of XW42 Tool Steel, *Journal Of Materials Processing Technology*, **2008**, **201**, 570-573, doi:10.1016/j.jmatprotec.2007.11.285;
31. Berri, N., Maheshwari, S., Sharma, C., Kumar, A.: Performance Evaluation of Powder Metallurgy Electrode in Electrical Discharge Machining of AISI D2 Steel Using Taguchi Method, *International Journal of Mechanical and Mechatronics Engineering*, **2008**, **2** (2), 225-229;
32. Muttamara, A., Fukuzawa, Y., Mohri, N., Tanid, T.: Effect of Electrode Material on Electrical Discharge Machining of Alumina, *Journal of Materials Processing Technology*, **2009**, **209**, 2545-2552, doi:10.1016/j.jmatprotec.2008.06.018;
33. Pellicer, N., Ciurana J., Delgado, J.: Tool Electrode Geometry and Process Parameters Influence on Different Feature Geometry and Surface Quality in Electrical Discharge Machining of AISI H13 Steel, *Journal of Intelligent Manufacturing*, **2011**, **22**, 575-584, doi:10.1007/s10845-009-0320-81;
34. Muthuramalingam, T., Mohan, B.: Influence of Tool Electrode Properties on Machinability in Spark Erosion Machining, *Materials and Manufacturing Processes*, **2013**, **28** (8), 939-943, doi:10.1080/10426914.2013.763973;
35. Khan, M.A.R., Rahman, M.M.: An Experimental Investigation on Surface Finish in Die-sinking EDM of Ti-5Al-2.5Sn, *International Journal of Advanced Manufacturing Technology*, **2015**, **77**, 1727-1740, doi:10.1007/s00170-014-6507-y;
36. Younis, M.A., Abbas, M.S., Gouda, M.A., Mahmoud, F.H., Abd Allah, S.A: Effect of Electrode Material on Electrical Discharge Machining of Tool Steel Surface, *Ain Shams Engineering Journal*, **2015**, **6**, 977-986, doi:10.1016/j.asej.2015.02.001;

37. Kumar, S.S., Uthayakumar, M., Kumaran, S.T.: Electrical Discharge Machining of Al (6351) Alloy: Role of Electrode Shape, *International Journal of Materials and Product Technology*, **2016**, **53** (1), 86-97, doi:10.1504/IJMPT.2016.076378;
38. Bhaumik, M., Maity, K.: Effect of Different Tool Materials During EDM Performance of Titanium Grade 6 Alloy, *Engineering Science and Technology, an International Journal*, **2018**, **21** (3), 507-516, doi:10.1016/j.jestch.2018.04.018;
39. Rahul Mishra, D.K., Datta, S., Masanta, M.: Effects of Tool Electrode on EDM Performance of Ti-6Al-4V, *Silicon*, **2018**, **10**, 2263-2277, doi:10.1007/s12633-018-9760-0;
40. Bahgat, M.M., Shash, A.Y., Abd-Rabou, M., El-Mahallawi, I.S.: Influence of Process Parameters in Electrical Discharge Machining on H13 Die Steel, *Heliyon*, **2009**, **5**, e01813, doi:10.1016/j.heliyon.2019.e01813;
41. Gopal, R., Thangadurai, K.R., Thirunavukkarasu, K.: Behavior of ECAP Processed Copper Electrodes in Electrical Discharge Machining of AISI H13 Steel, *Materials Today: Proceedings*, **2020**, **21** (1), 295-298, doi:10.1016/j.matpr.2019.05.443;
42. Gu, L., Farhadi, A., Zhu, Y., He, G., Zhao, W., Rajurkar, K.: A Novel Tool Design Procedure for Arc Sweep Machining Technology, *Materials and Manufacturing Processes*, **2020**, **35** (1), 113-121, doi: 10.1080/10426914.2020.1711920;
43. Chandrashekarappa, M.P.G, Kumar, S., Jagadish, Pimenov, D.Y., Giasin, K.: Experimental Analysis and Optimization of EDM Parameters on HcHcr Steel in Context with Different Electrodes and Dielectric Fluids Using Hybrid Taguchi-Based PCA-Utility and CRITIC-Utility Approaches, *Metals*, **2021**, **11**, 419, doi:10.3390/met11030419;
44. Jiang, Y., Kong L., Ping X., Zhang, Y., Zhao, W.: Utilizing a Porous-electrode for the Flushing Fluid in Electrical Discharge Machining, *Journal of Manufacturing Processes*, **2021**, **62**, 248-256, doi:1016/j.jmapro.2020.12.012;
45. Jiang, Y., Kong, L., Yu, J., Hua, C., Zhao, W.: Experimental Research on Preparation and Machining Performance of Porous Electrode in Electrical Discharge Machining, *Journal of Mechanical Science and Technology*, **2022**, **36** (12), 6201-6215, doi:10.1007/s12206-022-1134-2;
46. Khoshaim, A.B., Muthuramalingam, T., Moustafa, E.B., Elsheikh, A.: Influences of Tool Electrodes on Machinability of Titanium α- β Alloy with ISO Energy Pulse Generator in EDM Process, *Alexandria Engineering Journal*, **2023**, **63**, 465-474, doi:1016/j.aej.2022.07.059;
47. https://www.matweb.com/, MatWeb, Your Source for Materials Information, accessed November 17th, 2023;
48. Tharian, B.K., Dhanish, P.B., Manu, R.: Investigation on the Impact of Sub-zero Treated Electrodes in EDM, *Materials and Manufacturing Processes*, **2023**, doi:10.1080/10426914.2023.2289673;
49. Tripathy, S., Tripathy, D.K.: Multi-attribute Optimization of Machining Process Parameters in Powder Mixed Electro-discharge Machining Using TOPSIS and Grey Relational Analysis, *Engineering Science and Technology, an International Journal*, **2016**, **19**, 62-70, doi:10.1016/j.jestch.2015.07.010.